The three dimensionality of triple quantum dot stability diagrams

2009 New J. Phys. 11 113037

(http://iopscience.iop.org/1367-2630/11/11/113037)

New Journal of Physics
The open-access journal for physics

The three dimensionality of triple quantum dot stability diagrams

M C Rogge[1] **and R J Haug**
Institut für Festkörperphysik, Leibniz Universität Hannover,
Appelstr. 2, 30167 Hannover, Germany
E-mail: rogge@nano.uni-hannover.de

New Journal of Physics **11** (2009) 113037 (10pp)
Received 4 August 2009
Published 20 November 2009
Online at http://www.njp.org/
doi:10.1088/1367-2630/11/11/113037

Abstract. We present the full three dimensionality of an electrostatically calculated stability diagram for triple quantum dots. The stability diagram maps out the favored charge configuration of the system as a function of potential shifts due to gate voltages. For triple dots only a three-dimensional visualization allows for the complete identification of all its components. Those are most notably the so-called quadruple points where four electronic configurations are degenerate, and quantum cellular automata processes. The exact positions of these features within the stability diagram are now revealed. Furthermore, the influence on transport is studied by comparing the model with a two-path triple quantum dot made with local anodic oxidation. The two-path setup allows us to study the influence of the dots' arrangement.

Contents

[1] Author to whom any correspondence should be addressed.

1. Introduction

The electronic properties of quantum dots have been studied for several decades now [1]. Since quantum dots have been proposed as crucial elements of future quantum information technologies [2], these systems have gained even more attention. First, single quantum dots were studied as they could be used to realize a quantum mechanical bit (qubit) based on the electronic spin. Soon also double quantum dots [3] came into focus. Due to technical and scientific improvements in recent years, the research on quantum dots finally reached a level allowing for the detailed analysis of coupled triple quantum dots (e.g. [4]–[9]). They represent the first step towards coupled qubit chains as they are needed for quantum computers. They can also work as single qubits themselves [10]. Other interesting applications can be built with triple quantum dots, e.g. charge rectifiers and ratchets [4, 11] or spin entanglers [12]. They can be used to study other effects like the Kondo and Aharonov–Bohm effects [13, 14] or dark states [15].

The first and most crucial requirement for high-level research on quantum dot systems is the understanding of the stability diagram. The stability diagram maps out the charge configuration of the system as a function of potential detuning and does not depend on the setup of transport leads (as long as there are no instabilities, see below). In particular, it shows degeneracy points, where several charge configurations are degenerate, a precondition for transport in multiple dot systems. For triple quantum dots the full complexity of the stability diagram can only be revealed in three dimensions. The degeneracy points consist of at least four degenerate configurations (quadruple points). Although any researcher is reliant on this map for exact analysis, these diagrams are still not well known. Parts of it were presented by Vidan *et al* [16] and also Stopa [11], but the presentations remain incomplete showing only the first quadruple point. Gaudreau *et al* [5] first discovered several quadruple points with four degenerate electronic configurations. Furthermore, they found quantum cellular automata (QCA) processes [17]–[19] leading to charge rearrangements in two dots, when an electron is added to the third dot. However, the diagram is presented in a two-dimensional visualization only, not capable of revealing the full properties. Schröer *et al* [6] showed a three-dimensional visualization, but due to the large number of electrons covered by this visualization, it is not possible to see the dynamics at triple dot resonances, namely the positions and properties of quadruple points. On vertical quantum dots Amaha *et al* [20] mapped out the stability diagram and also presented it in three dimensions, but the quadruple points are not resolved due to high temperatures. So even though the mathematics is well established and stability diagrams were calculated [5, 6, 16], measured [5]–[9], [20] and visualized [5, 6, 11, 16, 20], a complete and detailed three-dimensional stability diagram was never developed. This is a huge deficiency in the understanding of these systems. As a result false assumptions were made. For example Schröer *et al* [6] stated that the number of quadruple points is four. However, quadruple points do not feature four intersecting charging or charge reconfiguration planes but six. In addition, transport in a serial triple dot is possible not only at these quadruple points.

In this paper, we develop and visualize an electrostatic model for stability diagrams of triple quantum dots. Although the underlying mathematics is straightforward and does not differ considerably from other ansatzes, the model and its visualization goes far beyond existing models as it covers the full three dimensionality of these diagrams. Thus, it finally fills the aforementioned deficiencies. It allows for the complete analysis of its components, especially the intensively discussed quadruple points and the interplay with QCA processes. It is found that there are in general six quadruple points instead of only four. All six points can show sequential

transport. Furthermore, the QCA processes appear not only at certain points or lines as implied until now, but at a full plane in the center of the diagram. Depending on the arrangement of the quantum dots and the leads, the complete plane can contribute to transport.

The parameters for the model are chosen such that it compares to a real triple quantum dot, measured with transport and charge detection. This allows us to qualitatively study the influence of the model's features on transport, even though the real device shows finite tunnel coupling, which is not covered by the model. The two-path setup of the device allows us to understand the role of the dots' arrangement. From the two-path transport a single path transport can be calculated that nicely fits to the model's predictions.

2. Electrostatic model

For the calculation of the three-dimensional model of a triple dot charge diagram, we determine the energetically favored electronic configuration around the transition from zero electrons in the system to one on each dot (equivalent to any other total electron numbers from N to $N+1$ on each dot) for any given set of three gate voltages V_{G1}, V_{G2} and V_{G3} used for detuning the potential. The number of possible electronic configurations of a system containing M quantum dots is 2^M. The number of configurations for a total electron number N is $\binom{M}{N}$ with either zero or one electron on each dot. Thus, a triple dot has $2^3 = 8$ possible configurations (N_A, N_B, N_C) with N_A, N_B, N_C being the electron numbers for the three dots named A, B, C. There is one configuration for zero electrons in the system: (0, 0, 0), three for one electron: (1, 0, 0), (0, 1, 0), (0, 0, 1), three for two electrons: (1, 1, 0), (1, 0, 1), (0, 1, 1) and one for three electrons: (1, 1, 1). The electrostatic energies for these configurations as a function of gate voltages are

for zero electrons:

$$E_0 = 0,$$

for one electron on dot i:

$$E_i = \frac{-e}{C_{\Sigma i}} \left(C_{i1} V_{G1} + C_{i2} V_{G2} + C_{i3} V_{G3}\right),$$

for two electrons, one on dot i, one on dot j:

$$E_{i,j} = E_i + E_j + e^2 \frac{C_{ij}}{C_{\Sigma i} C_{\Sigma j}},$$

and for three electrons with one electron each on dots i, j, k:

$$E_{i,j,k} = E_{i,j} + E_{i,k} + E_{j,k} - E_i - E_j - E_k,$$

with $i, j, k \in \{A, B, C\}$, $i \neq j \neq k$. C_{i1}, C_{i2}, C_{i3} are the capacitances between dot i and gates 1, 2, 3 and $C_{\Sigma i}$ is the total capacitance of dot i. The capacitances C_{ij} reflect the capacitive interaction between dots i and j, that leads to anticrossings in stability diagrams. For any given set of gate voltages V_{G1}, V_{G2} and V_{G3}, the charge configuration is determined by calculating, which of the relevant energies is the lowest. So the stability diagram is completely covered. The adjustment to the measured triple dot is done by adjusting the capacitances.

An artistic view of the measured triple dot device is shown in figure 1. The sample is made by local anodic oxidation [21]–[23] on a GaAs/AlGaAs heterostructure. The oxide lines (black)

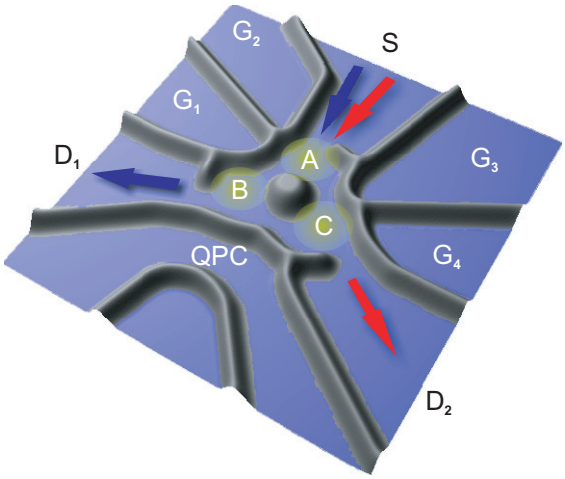

Figure 1. Artistic view of the measured triple quantum dot made with local anodic oxidation. Oxide lines (black) define three dots A, B, C coupled to Source (S), Drain1 (D1) and Drain2 (D2). The potentials are controlled via four gates G1, G2, G3 and G4. Transport is measured along two paths (blue and red arrows). A quantum point contact (QPC) serves for charge detection.

define three dots A, B and C, which are connected to three leads: Source (S), Drain1 (D1) and Drain2 (D2). Thus transport can be measured along two paths, from Source via dots A and B to Drain1 (blue arrows) and from Source via A and C to Drain2 (red arrows). A QPC is added for charge detection. The geometry of the device and the measurement technique is explained in full detail in [7, 8].

The upper part of figure 2 shows measurements on this device recorded using charge detection. This method does not depend on the setup of the leads (again as long as there are no instabilities) and is thus capable of measuring the stability diagram. As a function of gate voltages V_{G1} and V_{G3} several lines are visible denoting charge rearrangements of the system. Lines with a steep slope correspond to charging of dot C with an additional electron; those with a shallow slope correspond to charging of dot B. Intermediate slopes appear due to charging of dot A (see central measurement). The three shown measurements are cuts through the three-dimensional stability diagram in the vicinity of a resonance of all three dots. At $V_{G2} = -10\,\mathrm{mV}$ this resonance is not yet established. The system still acts as independent double dots. Three different anticrossings are visible that appear due to capacitive coupling for resonance of dots A–B, A–C and B–C, but those anticrossings are well separated. The same description applies for $V_{G2} = 10\,\mathrm{mV}$, except that the anticrossings have swapped places. However, this is different at the center image at $V_{G2} = 0\,\mathrm{mV}$. Here, all three anticrossings have merged. In the vicinity resonances of a triple quantum dot are expected, quadruple points form, and QCA processes take place.

How the observed features can be understood in detail is examined using the three-dimensional model. The capacitances needed to fit the model to the measurements are extracted from these and other measurements. The result is shown in the bottom part of figure 2. For the same voltages as in the measurements, the energetically lowest electronic configurations (N_A, N_B, N_C) are plotted in a color-encoded manner. With the chosen capacitances (see caption of figure 2) the model fits pretty well.

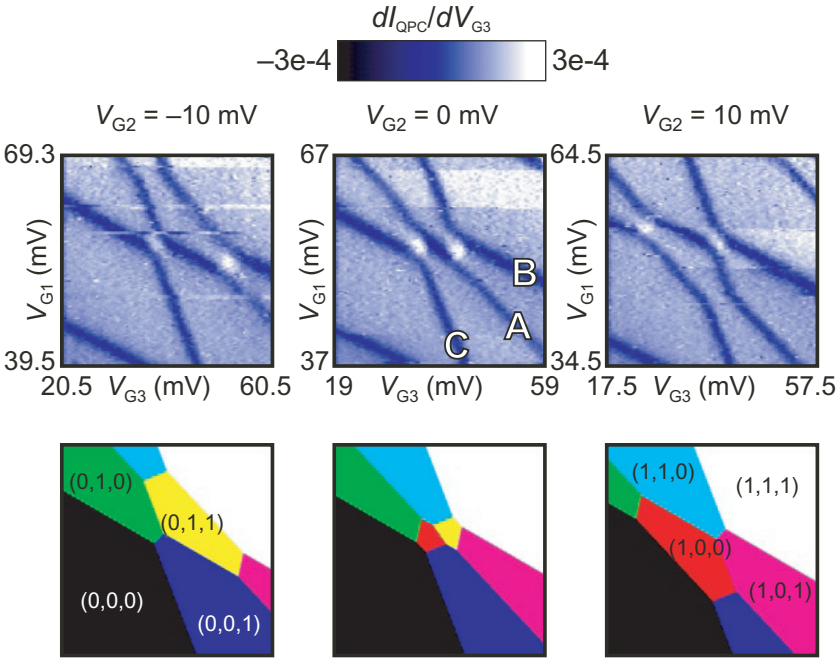

Figure 2. Upper panel: derivative of the QPC current I_{QPC} with respect to V_{G3} as a function of V_{G1} and V_{G3} for three different voltages at G2. Dark lines correspond to charging of dots A, B, C (see middle plot). For $V_{G2} = -10$ mV and $V_{G2} = 10$ mV anticrossings appear due to double dot physics, around $V_{G2} = 0$ mV, triple dot resonances are formed. Lower panel: electrostatic model for the upper cases using the following capacitances: $C_{\Sigma A} = 71.0$ aF, $C_{\Sigma B} = 98.2$ aF, $C_{\Sigma C} = 35.6$ aF, $C_{A1} = 6.2$ aF, $C_{A2} = 5.15$ aF, $C_{A3} = 5.0$ aF, $C_{B1} = 9.4$ aF, $C_{B2} = 3.8$ aF, $C_{B3} = 4.05$ aF, $C_{C1} = 1.5$ aF, $C_{C2} = 1.1$ aF, $C_{C3} = 3.0$ aF, $C_{AB} = 15.5$ aF, $C_{AC} = 6.8$ aF, $C_{BC} = 4.4$ aF.

3. Three-dimensional model visualization

The three images shown at the bottom of figure 2 are, as explained, cuts through the three-dimensional stability diagram. Even though the central image is a cut through the center of the diagram, right here no quadruple points appear. However, they are in the direct vicinity, close enough to be visible in measurements (like on the right side of figure 5) due to finite peak widths. To completely understand the model, a full three dimensional visualization is indispensable. This visualization is presented in figure 3. The stability diagram is shown from four different perspectives as a function of all three gate voltages. It is in general composed of three planes colored red, blue and green. At each of these planes the total charge of the system is changed by one electron which is added to a certain dot via the leads. The green (blue, red) plane corresponds to charging of quantum dot A (B, C). These planes intersect as they have different gradients. At these intersections double dot resonances are established. Due to the finite interdot capacitances the dots interact and thus the planes shift. Therefore, when two planes intersect, anticrossings are formed with three degenerate electronic configurations on each side. In two dimensions these degeneracies are called triple points. In three dimensions they are transformed

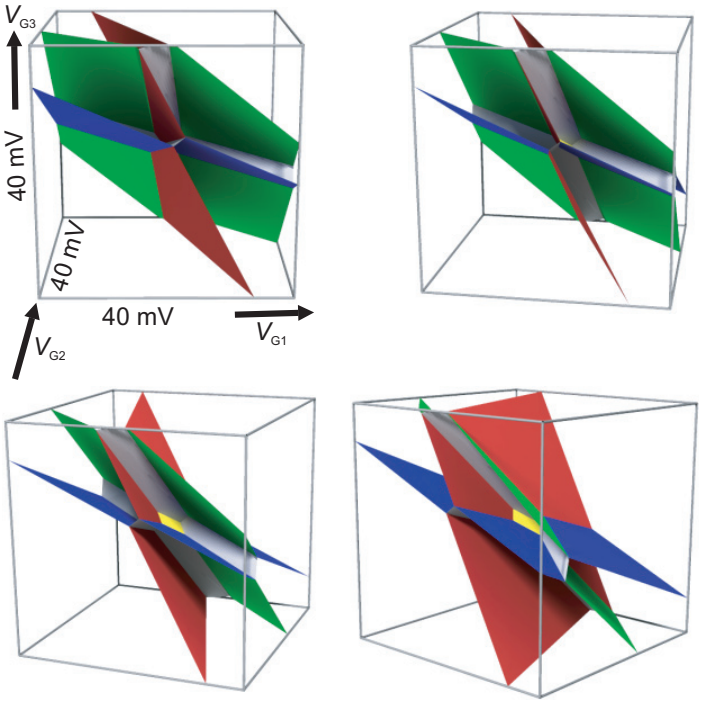

Figure 3. Three-dimensional stability diagram shown from four perspectives. Three planes (green for charging of dot A, blue for B, red for C) cross in the center of the model and shift due to finite coupling. Quadruple points are formed along with a central plane (yellow) featuring QCA processes.

into triple lines. A pair of triple lines is connected with a gray plane. At these planes an electron is moved from one dot to another without changing the total number of electrons in the system. The spaces between all the planes are characterized by stable electronic configurations.

At the center of the model the situation becomes more complex as now all three colored planes intersect. Here, quadruple points are expected as well as QCA processes. Indeed the model shows a feature that cannot be explained with double dot physics. In the center of the model another plane appears (colored yellow). This is shown in more detail in figure 4 where the center of the model is highlighted. The yellow plane is different to all other planes of the model. It has a different gradient and neither corresponds to charging of a certain dot only nor to pure charge rearrangements within the system. Instead it features both. At the whole plane the configurations (1, 0, 0) and (0, 1, 1) are degenerate. Thus the following process is possible: when there is one electron on dot A (1, 0, 0), a second electron can enter via dot B (C). At the same time the electron on dot A is shifted to dot C (B) leaving the system in the (0, 1, 1) configuration. This is a QCA process, one of the major discoveries in triple dot systems. It appears along the whole yellow plane.

This central plane is surrounded by points, where six planes (colored and gray) intersect. These are the so-called quadruple points that feature four degenerate charge configurations. Together with the QCA process, these points are the manifestation of the triple dot. Six quadruple points exist, two more than expected according to previous publications. There is one below the central plane (qp1), one above (qp6) and four more that actually define the central

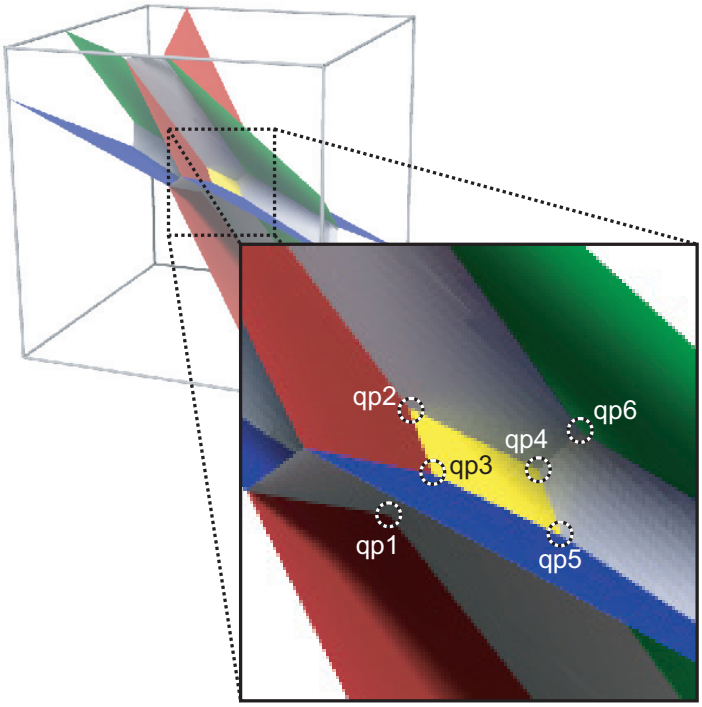

Figure 4. Highlighted center of the three dimensional stability diagram. The central yellow plane is defined by four quadruple points qp2, qp3, qp4 and qp5. Another one is below the plane (qp1) and above (qp6).

plane (qp2, qp3, qp4, qp5). Only under special conditions, the number of degeneracy points can be reduced. If for example the three dots do not interact, there is only one point, where all planes intersect with all eight charge configurations being degenerate. For the more general case of six quadruple points, four of them are already known. For those the following configurations are degenerate:

qp1: (0, 0, 0), (1, 0, 0), (0, 1, 0), (0, 0, 1),
qp2: (1, 0, 0), (0, 1, 0), (1, 1, 0), (0, 1, 1),
qp5: (1, 0, 0), (0, 0, 1), (1, 0, 1), (0, 1, 1),
qp6: (1, 1, 0), (1, 0, 1), (0, 1, 1), (1, 1, 1).

The two quadruple points qp3 and qp4 with degenerate configurations

qp3: (1, 0, 0), (0, 1, 0), (0, 0, 1), (0, 1, 1),
qp4: (1, 0, 0), (1, 1, 0), (1, 0, 1), (0, 1, 1),

have not been known so far, as they appear in a different way in two dimensional cuts through the stability diagram. For the other quadruple points even a two dimensional cut shows all four charge configurations that meet at the quadruple point. For qp3 and qp4, only three configurations meet at one point in two dimensions. The fourth configuration touches this point coming from the third dimension. So this point does not appear as a quadruple point in two dimensions. qp3 and qp4 were therefore overlooked.

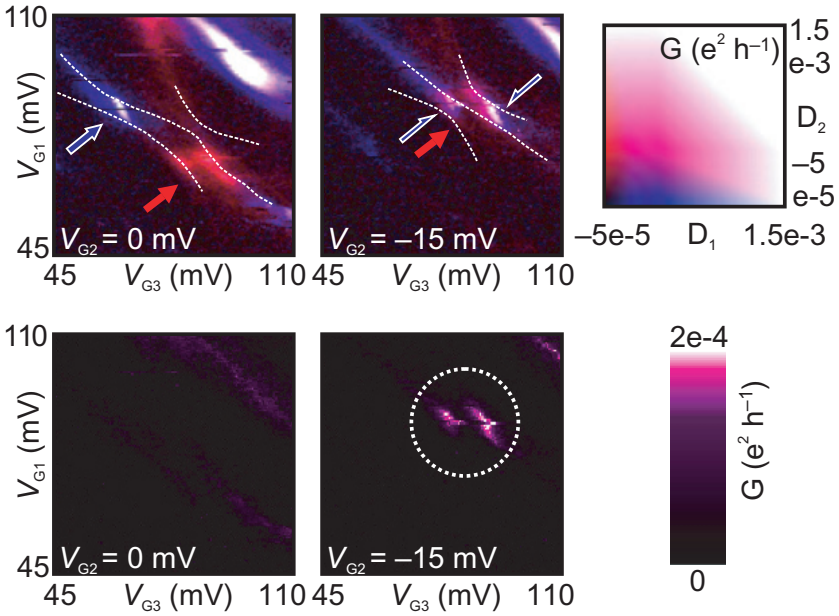

Figure 5. Upper panel: conductances along the two paths (path1 in blue, path2 in red) as a function of V_{G1} and V_{G3} off (left) and on (right) triple dot resonance. Features from double and triple dot physics are visible. Lower panel: from measured transport calculated hypothetic serial conductance. Double dot features vanish, only triple dot resonances remain. They appear as a two-spot feature (dashed circle).

4. Comparison with transport measurements

As mentioned before, the properties of the stability diagram (and of charge detection) do not depend on how the dots are connected to the leads. In particular, they do not depend on the transport paths. This is not true for the conductance properties. They strongly depend on the dots' arrangement. With the model now well known the transport properties of our two-path triple quantum dot can be analyzed. The upper part of figure 5 shows two transport measurements as a function of V_{G1} and V_{G3}. The conductance of both transport paths is plotted simultaneously, path1 in blue, path2 in red (results from charge detection are added as dashed lines). The left plot at $V_{G2} = 0$ mV corresponds to the back side of the three dimensional model. There is no resonance of all three dots. Nevertheless features are visible in both paths showing double dot resonances. The red features (marked with a red arrow) appear due to a resonance of dots A and C. They correspond to the triple lines on both sides of the anticrossing when the model's red and green planes intersect (see figure 2). Indeed one can see that the two involved triple lines form a double feature of two triple points in the measurement. The blue feature (blue arrow) corresponds to the intersection of the blue and the green planes from the model due to resonance of dots A and B. Although there are two triple lines involved as well, there is only one spot visible as the anticrossing is not large enough and cannot be resolved in transport. The right plot at $V_{G2} = -15$ mV corresponds to the center of the model. Here resonances of all three dots appear. This becomes obvious as both paths show transport at the same time. Quadruple points must be involved. But the exact spots of triple dot resonances are not clearly visible, as

the measurement still shows features from double dots. However, due to the two-path setup, there is an elegant way to separate the triple dot features.

Assuming the two paths to be ohmic with conductances G1 and G2, one can calculate a hypothetic transport from Drain1 via dots B, A, C to Drain2. Thus, the arrangement of the dots can be mathematically changed to form three dots in series with a combined conductance $G = 1/(1/G1 + 1/G2)$. Such an arrangement can only show transport if all three dots are resonant. Therefore, double dot features should be wiped out. Of course this method does not include nonohmic effects. Furthermore the tunnel resistance to the Source is still included which is not the case in a real serial device. Finally the real arrangement is of course unchanged. The observed features must still be analyzed in terms of the two-path setup.

The result of this method is presented in the lower panel of figure 5 for both voltages V_{G2}. Indeed the double dot features are strongly suppressed. For $V_{G2} = 0\,\mathrm{mV}$ almost no conductance is visible. All the triple points have disappeared. For $V_{G2} = -15\,\mathrm{mV}$ transport is suppressed as well. However, two spots are left (dashed circle). These are the features from the triple dot that appear now well separated.

As the conductance properties depend on the dots' arrangement, it is not guaranteed that all quadruple points can contribute to transport. However, the quadruple points qp1 and qp6 are always visible as long as there are at least two leads connected to three coupled dots. At qp1 an electron can enter the empty system at any dot that is connected to a lead. It can then travel from dot to dot until it reaches the exit lead. The same occurs at qp6 for holes. Quadruple points qp2 to qp5 are not that trivial. For the two path setup, transport means charge exchange between the Source lead and one or both Drain leads. This is possible at qp2 and qp5. At qp2, transport in path1 can occur via the transition $(1, 0, 0) \rightarrow (1, 1, 0) \rightarrow (0, 1, 0) \rightarrow (1, 0, 0)$. An electron can enter from Drain1 to dot B, another electron then leaves via dot A to Source and the remaining electron shifts from B to A. The analogue process is possible for a hole in path2 with the transition $(0, 1, 1) \rightarrow (0, 1, 0) \rightarrow (1, 1, 0) \rightarrow (0, 1, 1)$. Similarly, transport is possible at qp5 in both paths via $(0, 1, 1) \rightarrow (0, 0, 1) \rightarrow (1, 0, 1) \rightarrow (0, 1, 1)$ in path1 and via $(1, 0, 0) \rightarrow (1, 0, 1) \rightarrow (0, 0, 1) \rightarrow (1, 0, 0)$ in path2. At qp3 and qp4 no transport is possible for the two-path setup. At both quadruple points neither electrons nor holes can enter the system via Source. So, the observed features in figure 5 must be quadruple points qp1, qp2, qp5 and qp6. According to the model, the quadruple points qp1 and qp2 are much closer than, e.g. qp1 and qp5. The same accounts for qp5 and qp6. So there are two pairs of quadruple points. Indeed, the measurements shows only two spots instead of four. They correspond to these two pairs. The quadruple points within a pair are again too close to be resolved. The left spot contains qp1 and qp2, the right spot contains qp5 and qp6. The observation of these pairs confirms the model nicely.

The gap between the two pairs also confirms that the real dot arrangement is of course not changed by the calculation of a hypothetical serial transport. For a real serial system with Source and Drain at dots B and C, transport would occur along the whole central plane via the QCA process (and via sequential tunneling at qp3 and qp4). As this process does not involve charge exchange with the Source lead, it does not produce transport in our device.

Even these stability diagrams can have instabilities. If for example there is only one lead attached to dot A at one end of a triple dot chain A, B, C, the configuration (1, 0, 0) could not be transferred directly to (0, 0, 1) even if both were degenerate. One had to lift this degeneracy to transfer the electron from A to B and from B to C. Then the degeneracy could be established again with the system in (0, 0, 1). So the actual charge configuration depends on the path through

the stability diagram. Such instabilities could appear in quadruple quantum dots even when two leads are attached.

5. Conclusion

In conclusion we have visualized the full three dimensionality of triple dot stability diagrams. We have developed an electrostatic model that was fit to match the properties of a triple dot device with a two-path setup. Due to the full visualization we were able to completely analyze all the model's features for triple dots. We found the maximum number of quadruple points (and degeneracy points in general) to be six instead of four as reported in other publications. We identified QCA processes that occur along a whole plane in the center of the model. The comparison with the two-path triple dot confirms the model and is capable of explaining all features visible in transport. Due to the two-path setup, we were able to separate double dot features from triple dot features. As a result, the transport properties in triple dots strongly depend on the dots' arrangement. Under certain circumstances transport is possible not only at quadruple points but along the whole central plane using the QCA process.

Acknowledgments

For the heterostructure, we thank M Bichler, G Abstreiter and W Wegscheider. This work was supported by BMBF via nanoQUIT.

References

[1] Kouwenhoven L P *et al* 1997 *Mesoscopic Electron Transport (NATO ASI Ser. E* vol 345) ed L L Sohn, L P Kouwenhoven and G Schön (Dordrecht: Kluwer) pp 105–214
[2] Loss D and DiVincenzo D P 1998 *Phys. Rev.* A **57** 120
[3] van der Wiel W G *et al* 2003 *Rev. Mod. Phys.* **75** 1
[4] Vidan A, Westervelt R M, Stopa M, Hanson M and Gossard A C 2004 *Appl. Phys. Lett.* **85** 3602
[5] Gaudreau L *et al* 2006 *Phys. Rev. Lett.* **97** 036807
[6] Schröer D *et al* 2007 *Phys. Rev.* B **76** 075306
[7] Rogge M C and Haug R J 2008 *Phys. Rev.* B **77** 193306
[8] Rogge M C and Haug R J 2008 *Phys. Rev.* B **78** 153310
[9] Amaha S *et al* 2008 *Physica* E **40** 1322
[10] Hawrylak P and Korkusinski M 2005 *Solid State Commun.* **136** 508
[11] Stopa M 2002 *Phys. Rev. Lett.* **88** 146802
[12] Saraga D S and Loss D 2003 *Phys. Rev. Lett.* **90** 166803
[13] Sakano R and Kawakami N 2005 *Phys. Rev.* B **72** 085303
[14] Kuzmenko T, Kikoin K and Avishai Y 2006 *Phys. Rev. Lett.* **96** 046601
[15] Michaelis B, Emary C and Beenakker C W J 2006 *Europhys. Lett.* **73** 677
[16] Vidan A, Westervelt R M, Stopa M, Hanson M and Gossard A C 2005 *J. Supercond.* **18** 223
[17] Lent C S, Tougaw P D, Porod W and Bernstein G H 1992 *Nanotechnology* **4** 49
[18] Amlani I *et al* 1999 *Science* **284** 289
[19] Toth G and Lent C S 2001 *Phys. Rev.* A **63** 052315
[20] Amaha S *et al* 2009 *Appl. Phys. Lett.* **94** 092103
[21] Ishii M and Matsumoto K 1995 *Japan. J. Appl. Phys.* **34** 1329
[22] Held R, Lüscher S, Heinzel T, Ensslin K and Wegscheider W 1999 *Appl. Phys. Lett.* **75** 1134
[23] Keyser U F, Schumacher H W, Zeitler U, Haug R J and Eberl K 2000 *Appl. Phys. Lett.* **76** 457